Journal of Modern Optics
Vol. 53, Nos. 1–2, 10–20 January 2006, 173–183

Taylor & Francis
Taylor & Francis Group

Resonant energy absorption of rare-gas clusters in strong laser pulses

ULF SAALMANN*
Max Planck Institute for the Physics of Complex Systems,
Nöthnitzer Str. 38, 01187 Dresden, Germany

(*Received 22 March 2005; in final form 2 May 2005*)

The ionization dynamics of rare-gas clusters in strong femtosecond laser pulses is studied microscopically by means of classical molecular dynamics using a hierarchical tree code. Systematic investigations for laser pulses from 25 to 400 fs duration have shown a transition from field ionization to resonant excitation of a collective motion of the cluster electrons. The latter effect is associated with a strong energy absorption and can be microscopically identified by examining the phase lag of the electron oscillation with respect to the laser field. The optimal conditions depend, via the expansion time, strongly on the cluster size, which was varied from 10^2 up to 10^4 atoms.

1. Introduction

Irradiation of atomic clusters by intense laser light became a domain of active research shortly after the advent of high-power lasers [1–3]. Exhaustive investigations of intense laser–cluster interactions [1–12] have consistently shown a greatly enhanced absorption of energy from the laser compared with the situation where the laser is focused into a gas of single atoms. This enhancement becomes possible due to the high atomic density in the cluster allowing for strong local charging with the arising electric fields, multiple electron–ion scattering associated with inverse-bremsstrahlung heating and collective effects such as resonant heating. The latter effect, which is the subject of this paper, typically requires rapid expansion of the cluster (i.e. during the laser pulse) in order to reach the resonance condition.

Therefore, the importance of one or the other heating mechanism should depend on the combination of cluster (size and type, i.e. mainly on the mass of the constituents) and laser pulse (peak intensity, duration, chirp). To obtain an insight into the absorption dynamics, pump–probe measurements [5, 7] and pulse length variation with a fixed pulse energy [6] have been used by measuring the ionization of a gas of clusters. These methods, although applied to different clusters, have consistently shown an optimum for the pulse length or the delay (of a few hundred femtoseconds) with maximum absorption [5], particularly for high charge states [6],

*Email: us@mpipks-dresden.mpg.de

Journal of Modern Optics
ISSN 0950–0340 print/ISSN 1362–3044 online
http://www.tandf.co.uk/journals
DOI: 10.1080/09500340500167701

or increased kinetic energy of the fragment ions [7]. This favours a *resonant* heating mechanism to be responsible for the enhanced ionization for a particular pulse duration.

Such a resonant mechanism was first proposed for large clusters (of more than 10^5 atoms) by Ditmire *et al*. [13]. In this phenomenological model, electrons inside the cluster are considered as 'small plasma balls' [13] confined by the ionic space charge. They are heated by the laser, resulting in partial ionization and expansion of the cluster due to hydrodynamic pressure. In the course of this expansion the electron density $\rho(t)$ and, consequently, the plasma frequency $\omega_p(t) \propto (\rho(t))^{1/2}$ decreases. This leads to strong energy absorption at resonance, where $\omega_p(t) = \omega$, with ω the laser frequency. The assumption of a homogeneous density $\rho(t)$ over the cluster volume can be relaxed [14], allowing for a radial dependence of the density $\rho(r, t)$. The dominant absorption mechanism is then seen to be resonant absorption at the cluster's surface where the density is of the critical value. This resonance moves inward and is maintained for a long time (typically for the whole pulse of a few hundred femtoseconds) until the maximum of the density in the inner part of the cluster falls below this value [14].

Besides these phenomenological models, microscopic simulations of the laser–cluster interaction [15] have shown resonant energy absorption for medium-size clusters (with about 10^3 atoms). In this case, the clusters are more highly charged and expand due to Coulomb repulsion. The electron dynamics is determined by the binding potential of the ions, which is approximately harmonic inside the cluster. Therefore, the dynamics in such a cluster can be well characterized by a simple model of a driven damped harmonic oscillator, which describes the dipole response of the electrons inside the cluster. We will show below that this characteristic feature applies to a wide range of cluster sizes and pulse energies. After briefly describing the theoretical model (section 2) we will present systematic calculations for various cluster sizes n and laser pulses (section 3).

2. Microscopic model

Our approach treats the classical dynamics of electrons and ions driven by a laser field [15] and is similar to those used previously for studying intense laser–cluster interactions [16–19]. The key idea of the numerical implementation is the division of bound electrons, not treated explicitly, and free electrons, treated by classical molecular dynamics. This means that the ionization process in (sufficiently large) clusters consists of two steps: inner and outer ionization.

2.1 *Inner ionization*

Inner ionization is the excitation of electrons from their atomic bound states, resulting in so-called quasi-free electrons. Numerically, this corresponds to the creation of new electrons whereby the rate may be determined using the ADK tunneling formula [20] and the electron-impact cross sections using the Lotz formula [21]. For the case of clusters, however, the Coulomb field of the neighbouring ions and electrons has to be taken into account for a proper description of

the inner ionization process. This is difficult for methods using rate equations and not free of additional parameters. In order to avoid these complications and to incorporate the effects of the environment, we describe the inner ionization classically [15]: an electron is 'created' at a particular ion with the correct binding energy if there is no other electron bound to that ion. This approach relies only on the top-to-bottom assumption of inner ionization [22] and includes barrier-suppression and electron-impact ionization without additional assumptions.

2.2 *Outer ionization*

Outer ionization is a subsequent step since electrons that are no longer bound by a particular atom/ion may still be held back by the cluster as a whole due to the large space charge. These electrons, which we call quasi-free, may be further heated until they end up in the continuum. This process is studied by the propagation of their classical equations of motion. However, for the cluster sizes of interest here ($n > 100$), traditional propagation schemes fail due to their unfavourable n^2 scaling. Hierarchical tree codes [23], however, scale typically as $n \log n$ and can be easily parallelized. We started from a gravitational n-body code [24] and adapted it to the case of Coulomb interacting particles with positive and negative charges. The code allows us to follow the dynamics of all charged particles over a few hundred femtoseconds with typical time steps of attoseconds. Alternatively, one can start from the particle-in-cell concept to handle clusters of this size [25].

3. Results and discussion

In this section, we will present investigations for xenon clusters with sizes of $n \sim 10^2 - 10^4$ atoms subjected to linearly polarized laser pulses at a wavelength of $\lambda = 780\,\mathrm{nm}$ with a Gaussian pulse shape

$$\mathcal{E}(t) = \sqrt{I/I_0}\, \mathrm{e}^{-\ln 2(2t/T)^2} \cos(\omega t), \tag{1}$$

where $I_0 = 3.5 \times 10^{16}\,\mathrm{W/cm^2}$. In order to facilitate the presentation of the results for the various peak intensities I and pulse durations T we list in table 1 the parameters used in the calculations below.

Table 1. List of laser peak intensities I in $\mathrm{W/cm^2}$ used in the calculation for different pulse durations T. The pulse energy is equal for all pulses in a row and increases by a factor of 5 from one row to the next.

	T (fs)				
	25	50	100	200	400
Set A	3.2×10^{15}	1.6×10^{15}	8×10^{14}	4×10^{14}	2×10^{14}
Set B	1.6×10^{16}	8×10^{15}	4×10^{15}	2×10^{15}	1×10^{15}
Set C	8×10^{16}	4×10^{16}	2×10^{16}	1×10^{16}	5×10^{15}

3.1 *Optimal pulse length*

First of all, we present in figure 1 the pulse length dependence of the ionization efficiency, quantified by the average charge q of the ionic fragments of the exploding clusters at the end of the applied laser pulse. It was obtained by counting the number of electrons which are inner *and* outer ionized. This pulse length dependence changes considerably with the cluster size (different panels of figure 1) and the pulse energy (different symbols in figure 1). However, if one compares the behaviour of smaller clusters in weaker fields (circles in the left panel) with that of larger clusters in stronger fields (squares in the middle panel and diamonds in the right panel) the curves are similar, showing a clear maximum for pulse lengths T between 100 and 200 fs. Furthermore, the maximal average charge is similar, namely $q \approx 7 \pm 1$.

For more energetic pulses (set C, cf. table 1) the maximum shifts towards shorter pulses, and for less energetic pulses (set A) it shifts towards longer pulses. In extreme cases the maxima are out of the range of the pulse duration studied and the curves are monotonically increasing or decreasing. Note that, in all three graphs of figure 1, the peak intensities decrease from the left to the right. Thus, we would expect that, as for the case of single atoms, lower intensities induce lower charge states. This can indeed be observed for Xe_{135} at the highest pulse energy (set C). However, the opposite behaviour is seen for Xe_{9093} at the lowest pulse energy (set A), where the weaker but longer pulses lead to stronger ionization. This can be interpreted as a transition from atomic or molecular ionization to cluster dynamics with collective effects.

This behaviour is summarized in figure 2. Obviously, the dynamics of the larger clusters in strong fields resembles those of smaller clusters in weaker fields. The limited data points, however, do not allow for absolute scaling relations.

3.2 *Ionization dynamics*

The existence of an optimal pulse length for ionization can be attributed to a resonant energy absorption of the clusters occurring when the laser pulse has reached its maximum at time $t = 0$. This mechanism applies to the quasi-free electrons which oscillate back and forth in the combined potential of cluster and laser field. Assuming a spherical, uniformly charged cluster with total charge Q_t and radius R_t the cluster potential reads

$$V_t(r) = \begin{cases} -Q_t(3R_t^2 - r^2)/(2R_t^3) & \text{if } r \le R_t, \\ -Q_t/r & \text{if } r \ge R_t. \end{cases} \tag{2}$$

The index t indicates that the charge and size of the cluster and thus the potential itself may change in time during the pulse. This proceeds 'adiabatically', i.e. much slower than the laser field oscillation. Resonance occurs if the eigenfrequency and the laser frequency are equal, $\Omega_t = \omega$, where the eigenfrequency for small-amplitude oscillations of the electron cloud is given by $\Omega_t^2 = Q_t/R_t^3$, which follows from the potential (2).

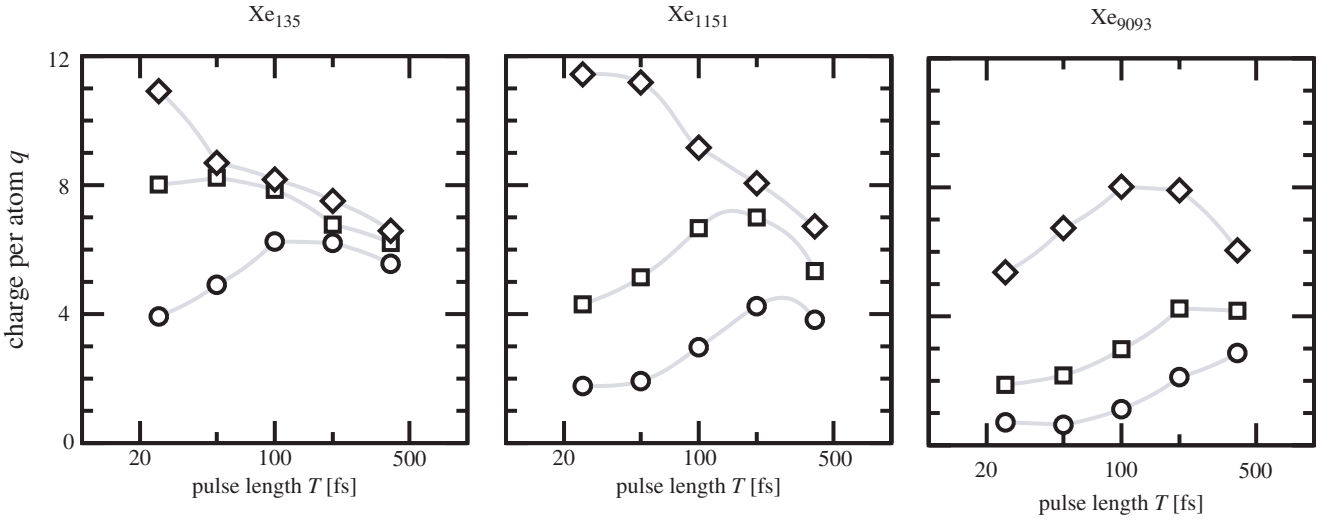

Figure 1. Average charge per atom for Xe_n clusters of three different sizes ($n = 135$, 1151 and 9093) as a function of the pulse length T or the peak intensity I. The energy of the pulse, i.e. the product $I \times T$, is kept constant for each curve. The three curves shown correspond to the intensities listed in table 1: set A (circles), set B (squares), and set C (diamonds).

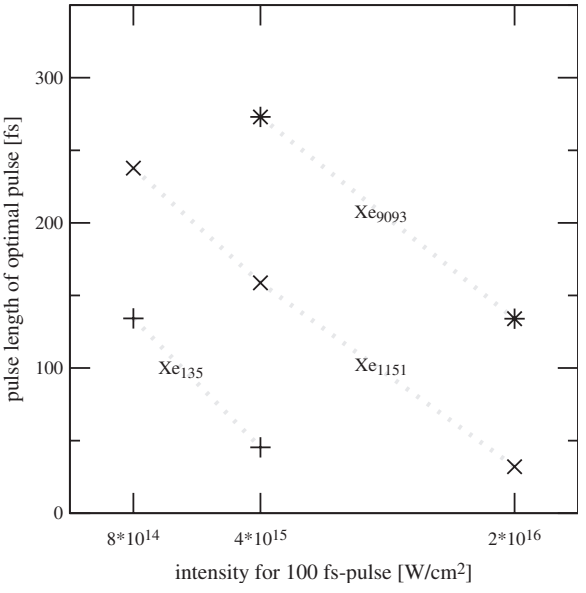

Figure 2. Optimal pulse length for the same three clusters as shown in figure 1. They are obtained from the maxima of the interpolating curves for the average charge per atom in that figure. Different symbols correspond to different cluster sizes Xe_n.

One can model the dynamics of the electron cloud (or more precisely that of the centre-of-mass position denoted by X) by a harmonic oscillator [15]

$$\ddot{X}(t) + 2\Gamma_t \dot{X}(t) + \Omega_t^2 X(t) = F(t). \tag{3}$$

Besides the harmonic potential term, we have introduced a damping term Γ_t, which accounts for collisions with ions and energy transfer to bound electrons as well as for the loss of high-energetic electrons to the continuum. Both effects damp the collective oscillation.

For periodic driving $F(t) = F_0 \cos(\omega t)$ the dynamics is explicitly given by [26]

$$X(t) = A_t \cos(\omega t - \varphi_t), \tag{4a}$$

$$\text{with} \quad A_t = \frac{F_0}{\sqrt{(\Omega_t^2 - \omega^2)^2 + (2\Gamma_t \omega)^2}}, \tag{4b}$$

$$\text{and} \quad \varphi_t = \arctan(2\Gamma_t \omega / (\Omega_t^2 - \omega^2)). \tag{4c}$$

Having the explicit solution (4), one can write the energy transfer to and from the oscillatory motion, which is

$$\langle \dot{E} \rangle = \langle \dot{E}_{\text{gain}} \rangle + \langle \dot{E}_{\text{loss}} \rangle, \tag{5a}$$

$$\text{with} \quad \langle \dot{E}_{\text{gain}} \rangle = \frac{1}{2} F_0 \, \mathrm{A}_t \, \omega \, \sin \varphi_t, \tag{5b}$$

$$\text{and} \quad \langle \dot{E}_{\text{loss}} \rangle = -\Gamma_t \, \mathrm{A}_t^2 \, \omega^2. \tag{5c}$$

The symbol $\langle \cdots \rangle$ denotes averages over a laser cycle. Whereas the loss or damping term is always negative, the pumping or gain term is positive for phase shifts $\varphi_t = 0 \ldots \pi$ and maximal at resonance $\varphi_t = \pi/2$. Furthermore, the phase shift is a good candidate to characterize the dynamics [15] since it passes $\pi/2$ at resonance, cf. equation (4c), independent of any additional parameter (such as the damping Γ_t) apart from the eigenfrequency Ω_t.

We will show below that this simple model describes surprisingly well the collective dynamics obtained from the microscopic calculations for the whole range of cluster sizes and laser pulses studied. This is not trivial since both the ionic structure and the Coulomb tail outside the cluster, cf. equation (2), are taken into account in the model equation of motion (3) only indirectly via the damping term Γ_t. Besides, nonlinear effects [27] are not contained in the model.

Figures 3 and 4 show the absorbed energy E as a function of time t along with the phase shift φ_t between the collective oscillation and laser field, cf. equation (4a). In order to eliminate the (trivial) time dependence of the energy absorption on the

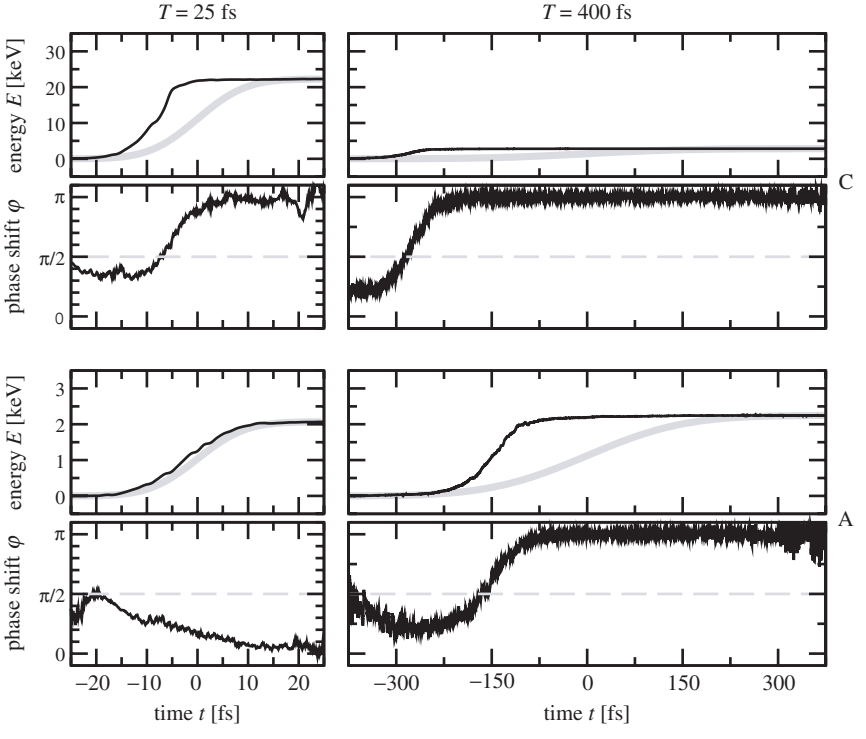

Figure 3. Absorbed energy per atom E and phase shift φ of collective electron motion in Xe_{135} with respect to the laser field as a function of time t. Both quantities are shown for four different laser pulses with durations of $T = 25$ fs and $T = 400$ fs, respectively, from the sets A and C in table 1. For the reference curves (gray solid lines) we assumed that the energy absorption is proportional to the instantaneous field strength of the laser, cf. equation (1). The motion is resonant for $\varphi = \pi/2$ (gray dashed lines).

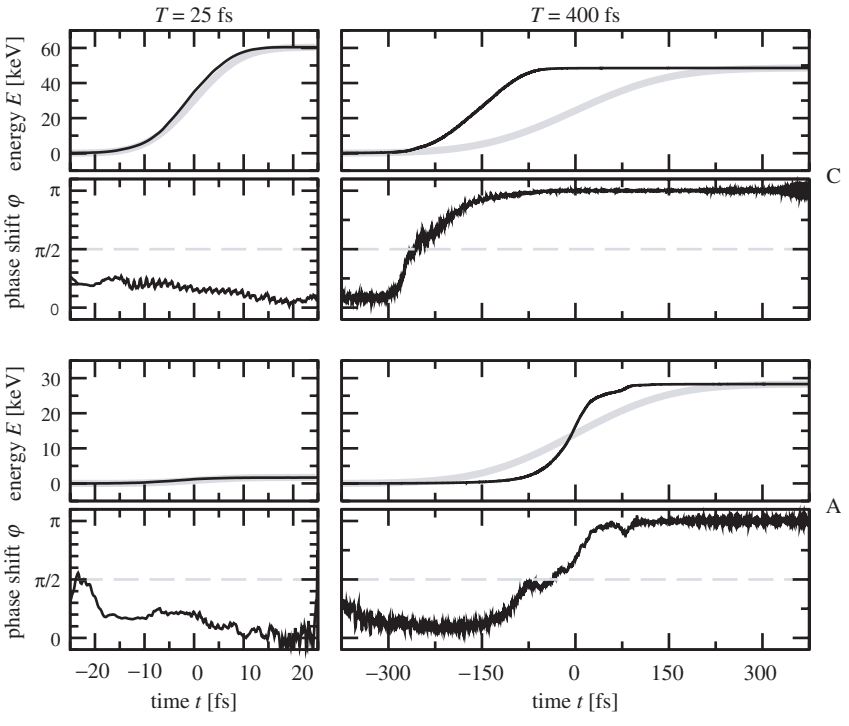

Figure 4. Same as figure 3 but for Xe_{9093}.

pulse shape, i.e. the instantaneous field strength, we plotted reference curves (gray lines in figures 3 and 4), which are obtained from energy absorption rates proportional to the Gaussian pulse shape (1). Integration yields $E_t \propto \mathrm{erf}(\ln 2(2t/T)^2)$. These curves are scaled to obtain the same final values for the absorbed energy $E_{t\to\infty}$ as obtained from the microscopic calculations. As can be seen from the figures, the actual absorption deviates strongly from the reference curves if the phase shift is $\varphi_t \approx \pi/2$. Around these times the increase, i.e. the absorption rate, is considerably higher.

Depending on the pulse duration we have two limiting scenarios. For shorter pulses the partially ionized clusters do not have enough time to expand into resonance, i.e. $\Omega_{t=0} > \omega$ and $\varphi_t \approx 0$. For the longer pulses the resonance has been passed before the pulse maximum, i.e. $\Omega_{t=0} < \omega$ and $\varphi_t \approx \pi$. In both cases the electric field is weak at resonance and thus the ionization reduced.

3.3 *Ionization mechanisms*

We have shown that the electron dynamics strongly depends on the pulse length. Now we examine the size dependence for short ($T = 25\,\mathrm{fs}$) and long ($T = 400\,\mathrm{fs}$) pulses. Since for the short pulses the clusters have no time to expand, they are, at least for pulse energies A and B, out of resonance. Assuming that the ionization in

this case is due to field ionization from a binding potential as given by equation (2), one can calculate the maximum charge state Q which can be reached for a given field strength $\mathcal{E}$ by requiring $\mathcal{E} = Q/R_0^2$. This follows from the situation where the barrier of the combined potential of the cluster (with R_0 the initial cluster radius) and laser vanishes [17]. Then, the maximal charge per atom is

$$q \propto \frac{\mathcal{E}}{R_0}. \tag{6}$$

Indeed, the average atomic charge q is inversely proportional to the cluster radius for the microscopic calculations, as can be seen in the left upper panel of figure 5. The curves according to equation (6), which are scaled by a common factor [28] in order to fit the highest charge in the figure, nicely agree with these data, confirming the assumption of field ionization for short pulses.

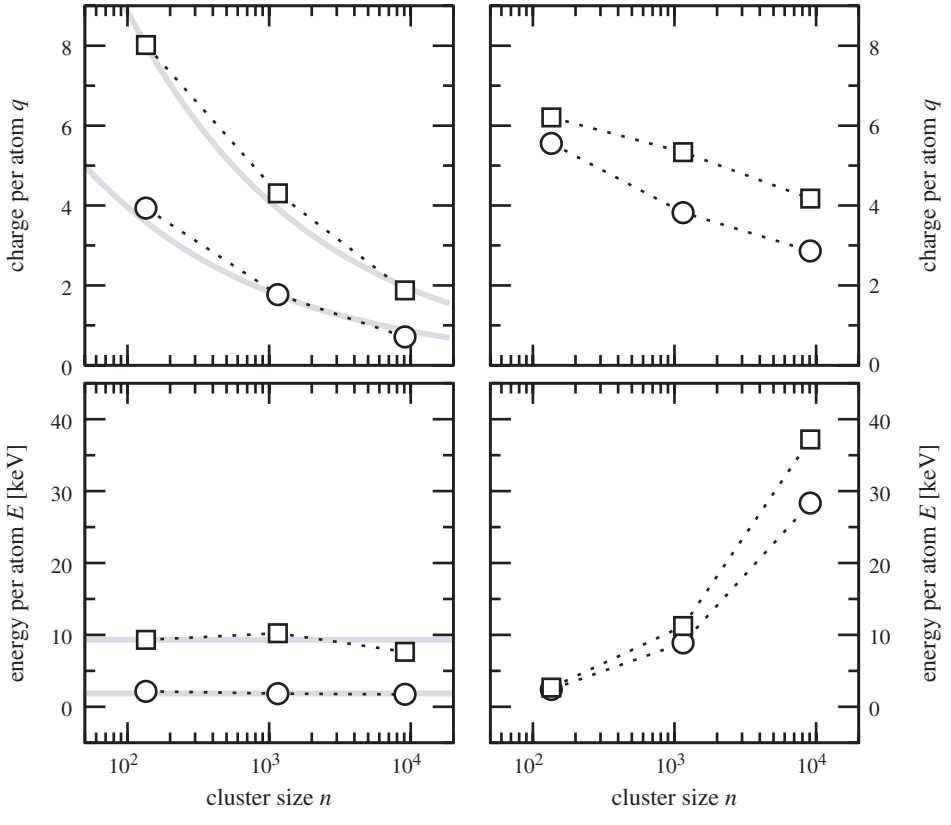

Figure 5. Charge (upper panels) and absorbed energy (lower panels) per atom as a function of the cluster size for 25 fs (left panels) and 400 fs (right panels) pulse length. The two sets of symbols correspond to the intensities listed in table 1: from row A (circles) and row B (squares). The gray lines show the expected charge, cf. equation (6), and energy, cf. equation (7), for the field ionization model discussed in the text.

The Coulomb energy of a uniformly charged sphere with total charge Q is $E = (3/5)Q^2/R$. From the above condition (6) for Q it follows that the energy per atom is

$$E \propto \mathcal{E}^2, \tag{7}$$

i.e. independent of the cluster radius/size. The lower left panel of figure 5 confirms that the transferred energy does not depend on the cluster size.

In order to achieve high-energetic explosions, one has to apply longer laser pulses to reach the optimal pulse length. In this case, as can be seen in the lower right panel of figure 5, much more energy is absorbed and finally converted into kinetic energy of the ions. In this regime, in contrast to the case of field ionization, larger clusters are more suitable for the production of fast fragment ions.

4. Summary

The efficiency of the strong-field ionization of rare-gas clusters depends critically on the pulse parameters. We found, in agreement with experimental data, an optimal pulse length for a given pulse energy. Whereas the actual value depends on the cluster size, the underlying mechanism, namely resonant excitation of the collective motion of electrons inside the cluster, applies to a wide range of cluster sizes. This has been confirmed by microscopic calculations which show a time-dependent phase shift of this collective oscillation with respect to the laser field. The strongest ionization is observed if the resonance occurs at the peak of the laser pulse.

Acknowledgments

Many helpful discussions with Jan M. Rost and a critical reading of the manuscript by Thomas Pattard are gratefully acknowledged.

References

[1] A. McPherson, B.D. Thompson, A.B. Borisov, *et al.*, Nature **370** 631 (1994).
[2] E.M. Snyder, D.A. Card, D.E. Folmer, *et al.*, Phys. Rev. Lett. **77** 3347 (1996).
[3] T. Ditmire, J.W.G. Tisch, E. Springate, *et al.*, Nature **386** 54 (1997).
[4] T. Ditmire, J. Zweiback, V.P. Yanovsky, *et al.*, Nature **398** 489 (1999).
[5] J. Zweiback, T. Ditmire and M.D. Perry, Phys. Rev. A **59** R3166 (1999).
[6] L. Köller, M. Schumacher, J. Köhn, *et al.*, Phys. Rev. Lett. **82** 3786 (1999).
[7] E. Springate, N. Hay, J.W.G. Tisch, *et al.*, Phys. Rev. A **61** 044101 (2000).
[8] V. Kumarappan, M. Krishnamurthy and D. Mathur, Phys. Rev. Lett. **87** 085005 (2001).
[9] Y. Fukuda, K. Yamakawa, Y. Akahane, *et al.*, Phys. Rev. A **67** 061201(R) (2003).
[10] K.Y. Kim, I. Alexeev, E. Parra, *et al.*, Phys. Rev. Lett. **90** 023401 (2003).
[11] E. Springate, S.A. Aseyev, S. Zamith, *et al.*, Phys. Rev. A **68** 053201 (2003).
[12] K.W. Madison, P.K. Patel, M. Allen, *et al.*, Phys. Rev. A **70** 053201 (2004).
[13] T. Ditmire, T. Donnelly, A.M. Rubenchik, *et al.*, Phys. Rev. A **53** 3379 (1996).
[14] H.M. Milchberg, S.J. McNaught and E. Parra, Phys. Rev. E **64** 056402 (2001).
[15] U. Saalmann and J.M. Rost, Phys. Rev. Lett. **91** 223401 (2003).

[16] C. Rose-Petruck, K.J. Schafer, K.R. Wilson, *et al*., Phys. Rev. A **55** 1182 (1997).
[17] I. Last and J. Jortner, Phys. Rev. A **60** 2215 (1999).
[18] K. Ishikawa and T. Blenski, Phys. Rev. A **62** 063204 (2000).
[19] Ch. Siedschlag and J.M. Rost, Phys. Rev. A **67** 013404 (2003).
[20] M.V. Ammosov, N.B. Delone and V.P. Krainov, Zh. Eksp. Teor. Fiz. **91** 2008 (1986).
[21] W. Lotz, Z. Phys. **206** 205 (1967); W. Lotz, Z. Phys. **216** 241 (1968).
[22] The most weakly bound electron is ionized first, which is in contrast to strong X-ray interaction with atoms/clusters, where predominantly inner-shell electrons are ionized by the laser. See U. Saalmann and J.M. Rost, Phys. Rev. Lett. **89** 143401 (2002).
[23] S. Pfalzner and P. Gibbon, *Many-body Tree Methods in Physics* (Cambridge University Press, Cambridge, 1996).
[24] J.E. Barnes and P. Hut, Nature **324** 446 (1986).
[25] C. Jungreuthmayer, M. Geissler, J. Zanghellini, *et al*., Phys. Rev. Lett. **92** 133401 (2004).
[26] L.D. Landau and E.M. Lifschitz, *Mechanics* (Pergamon Press, Oxford, 1994).
[27] S.V. Fomichev, D.F. Zaretsky, D. Bauer, *et al*., Phys. Rev. A **71** 013201 (2005).
[28] Using the atomic density of xenon, one could also calculate the absolute value of q. This value would be consistently smaller by a factor of 2.